Supporting Information

Temperature-dependent γ′ kinetics evolutions and elemental partitioning in a novel CoNi-based superalloy: An integrated CALPHAD phase-field experimental study

Table of contents

Supplemental Figure

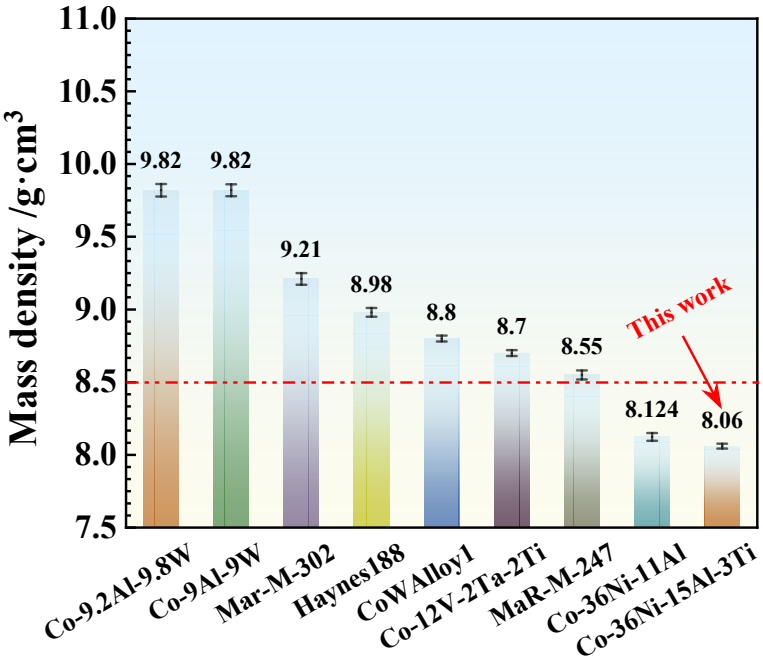

Fig. S1 Comparison of densities for the designed CoNi-based superalloy with Co-based and Ni-based superalloys.

2.2.3 Crystal plasticity model

The plastic deformation of fcc crystal is mainly through the dislocation slip on 12 octahedral <110> slip systems [1], so the plastic strain ε_{ij}^{p} can be calculated by the slip

accumulation of every activated slip system α in crystal plasticity model [3],

$$\varepsilon_{ij}^{p} = \sum_{\alpha} \gamma^{\alpha} m^{\alpha} \tag{15}$$

where ε_{ij}^{p} is the plastic strain rate, γ^{α} is the plastic shear rate on slip system α.

$m^{\alpha} = \frac{1}{2}(l^{\alpha} \otimes n^{\alpha} + n^{\alpha} \otimes l^{\alpha})$ is the Schmid tensor, l^{α} and n^{α} are respectively the unit vectors of the slip direction and the normal of slip plane.

γ^{α} follows the plastic flow rule and be written as,

$$\gamma^{\alpha} = \begin{cases} \gamma_0 \left(\dfrac{|\tau^{\alpha}|}{\tau_c^{\alpha}} \right)^m sign(\tau^{\alpha}), |\tau^{\alpha}| > \tau_c^{\alpha} \\ 0, |\tau^{\alpha}| < \tau_c^{\alpha} \end{cases} \tag{16}$$

where γ^{α} is the reference shear rate, τ_c^{α} is the critical resolved shear stress, and *m* is the plastic exponent, τ^{α} is the resolved shear stress. τ_c^{α} expounds the hardening behavior of the matrix and can be given by the interactions between different slip systems,

$$\tau_{c=}^{\alpha} \sum_{\beta} q^{\alpha\beta} h_0 \left(1 - \frac{\tau_c^{\beta}}{\tau_s} \right)^{\alpha} |\gamma^{\beta}| \tag{17}$$

where $q^{\alpha\beta}$ is the latent hardening parameter, h_0 is the initial hardening rate, τ_s is the saturated critical resolved shear stress, and *a* is the hardening exponent.

The plastic deformation in the soft γ matrix under external stress is mainly generated by the movement of octahedral slip systems 1/2<110> [1], so the 12 octahedral slip systems are considered in current model, S1($\bar{1}11$)[$0\bar{1}1$], S2($\bar{1}11$) [101], S3($\bar{1}11$)[110], S4(111)[$0\bar{1}1$], S5(111) [$\bar{1}01$], S6(111) [$\bar{1}01$], S7($\bar{1}\bar{1}1$)[011], S8($\bar{1}\bar{1}1$)[101], S9($\bar{1}\bar{1}1$)[$\bar{1}10$], S10($1\bar{1}1$)[011], S11($1\bar{1}1$)[$\bar{1}01$], and S12($1\bar{1}1$)[110]. The performance of 12 slip systems is predicted on the basis of the resolved shear stress τ^{α}. In the 2D simulation, some slip systems do not include the stress component in the direction of external stress, they are ignored due to the small contribution to the total creep strain[3].

Numerical solution of phase-field model

To facilitate the numerical calculations, the time variables and other PF variables

are first dimensionless as follows, $t^*=L\Delta ft$, $\mathbf{r}^*=\frac{\mathbf{r}}{l}$, $k_i^*=\frac{k_i}{\Delta f l^2}$, $k_\eta^*=\frac{k_\eta}{\Delta f l^2}$, $\nabla^*=\frac{\partial}{\partial(r/l)}$, $M_i^*=\frac{V_m M_i}{Ll^2}$, $f_{ch}^*=\frac{f_{ch}}{\Delta f}$, $f_{el}^*=\frac{f_{el}}{\Delta f}$, and the parameters used in the PF simulations are listed in Table S1. The simulations were performed with grid length of $l = 1 \times 10^{-9}$ m in a cell 160 × 160 grids, and a time step of $\Delta t^* = 0.02$; the standardization constant of the free energy is $\Delta f = 6 \times 10^6$ Jm^{-3}. Substituting the dimensionless parameters into Eqs. (1) and (2) yield the dimensionless form of the equations,

$$\frac{\partial x_i(r^*,t^*)}{\partial t^*}=\nabla^*\left\{M_i^*\nabla^*\left[\left(\frac{\partial(f_{ch}^*+f_{el}^*)}{\partial x_i(r^*,t^*)}\right)-k_i^*(\nabla^*)^2x_i(r^*,t^*)\right]\right\},(i=Ni,Al) \quad (15)$$

$$\frac{\partial \eta_p(r^*,t^*)}{\partial t^*}=-\left[\left(\frac{\partial(f_{ch}^*+f_{el}^*)}{\partial \eta_p(r^*,t^*)}\right)-k_\eta^*(\nabla^*)^2\eta_p(r^*,t^*)\right],(p=1,2,3) \quad (16)$$

the kinetic equations are solved by the semi-implicit Fourier spectrum method after dimensionless quantization [1].

Table S1 Parameters used in the phase-field simulation.

Definition	Parameter	Value
Molar volume	V_m	7×10^{-6} m^3/mol[1]
Interfacial mobility	L	6×10^{-7} J/mol[1]
Diffusion constant	D_0	1.6×10^{-5} m^2/s [1]
Boltzmann constant k	k	1.3×10^{-23} J/K[4]
Activation energy	U	2.4 eV[4]
Double-well potential height	ω	2×10^{-7} J/m^3[4]
Material parameter	θ	8 [5]
gradient energy coefficients	k_i	9.4×10^{-11} J/m[5]
	k_y	1.1×10^{-7} J/m[5]

Elastic moduli for γ	C_{11}^{γ}	234 GPa [4]
	C_{12}^{γ}	184 GPa[4]
	C_{44}^{γ}	94 GPa[4]
Elastic moduli for γ′	$C_{11}^{\gamma'}$	231 GPa[4]
	$C_{12}^{\gamma'}$	191 GPa[4]
	$C_{44}^{\gamma'}$	91GPa[4]

[1] S. Shi, Y. Li, Z. Yan, S. Yang, Y. Ju, Crystal plasticity phase-field simulation of slip system anisotropy during creep of Co-Al-V monocrystal alloy under multidirectional strain, International Journal of Mechanical Sciences 227 (2022) 107436.

[2] A.L. Nishant Choudhary, A phase-field model of concurrent Suzuki segregation and partial dislocation glide, Computational Materials Science 246 (2024) 113021.

[3] Y. Shan, J. Song, S. Wang, K. Niu, X. Wu, X. Bian, S. Muhammad, Y. Li, Unveiling γ′ phase creep damage in multi-component Ni-based superalloys by crystal plasticity phase-field simulation, Journal of Materials Chemistry A 56 (2026) 2050-7488.

[4] Z. Wang, C. Liang, D. Wang, X. Yue, J. Li, X. Ding, Unveiling the Co effect on the temporal evolution kinetics of γ′ phase in Ni-Al-Co model superalloys via CALPHAD–informed phase field simulations, Acta Materialia 258 (2023) 119247.

[5] Y. Tsukada, T. Koyama, F. Kubota, Y. Murata, Y. Kondo, Phase-field simulation of rafting kinetics in a nickel-based single crystal superalloy, Intermetallics 85 (2017) 187-196.